Sulfur pair in silicon: ^{33}S electron-nuclear double resonance

A. B. van Oosten and C. A. J. Ammerlaan
Natuurkundig Laboratorium der Universiteit van Amsterdam, Valckenierstraat 65, 1018 XE Amsterdam, The Netherlands
(Received 6 July 1988)

Sulfur pairs in silicon are studied by electron paramagnetic resonance (EPR) and by ^{33}S electron-nuclear double resonance. The trigonal symmetry and electron spin $S=\frac{1}{2}$ are experimentally established. For magnetic field **B** parallel to the [111] pair axis, the EPR intensity is strongly reduced. This gives the spectrum its isotropic appearance. A value for the g anisotropy is reported. The ^{33}S nucleus experiences a large quadrupole effect. The nearly isotropic hyperfine interaction is consistent with an even-parity ground state. Two possible models for the valence electronic structure are discussed. The g anisotropies of S_2^+ and Se_2^+ are qualitatively explained.

I. INTRODUCTION

The chalcogens S, Se, and Te are well known to form complexes in silicon. The first observation of sulfur in Si was made by Carlson *et al.*[1] who reported two sulfur-related donor levels in Si. The sulfur pair was the first chalcogen complex to be identified. Its electron paramagnetic resonance (EPR) spectrum, reported by Ludwig,[2] consists of an apparently isotropic resonance with $g=2.0008$. Attempts by this author to observe ^{33}S electron-nuclear double resonance (ENDOR) failed, but stress measurements indicated an electron spin of $\frac{1}{2}$. The hyperfine interactions with the 0.74%-abundant ^{33}S nucleus, which has nuclear spin $I=\frac{3}{2}$, directly led to its identification as a pair of two equivalent sulfur atoms. Though such a pair obviously cannot have cubic symmetry, no g anisotropy could be detected in EPR. The symmetry of the pair could therefore not be determined.

A definite identification of the energy levels reported by Carlson, situated at 187.5 and 370.0 meV below the conduction-band edge, as the $S_2^{0/+}$ and the $S_2^{+/2+}$ levels, was obtained from infrared (ir) absorption, Hall effect, resistivity, and photoconductivity measurements by Krag *et al.*,[3] Camphausen *et al.*,[4] and Janzén *et al.*[5] Furthermore, these authors report consistency with trigonal symmetry. An extensive review of ir absorption results for chalcogen centers in silicon is given by Wagner *et al.*[6]

Wörner and Schirmer[7] reported the EPR spectrum of the completely analogous Se_2 pair, revealing a detectable anisotropy. Their data were consistent with trigonal symmetry, but do not exclude a still-lower symmetry. The analogous Te_2 pair, which is known to exist from ir absorption,[6] has not yet been identified in EPR.

The double-donor character of the isolated and paired chalcogens indicates that the chalcogens occupy the substitutional lattice position, though Niklas and Spaeth[8] express some preference for the interstitial site for the isolated Te donor on the basis of a line-shape analysis. Recent calculations by Beeler *et al.*[9] provide evidence for the substitutional site. The parity of the ground state under space inversion has been the subject of some discussion. Wörner and Schirmer[7] concluded negative parity from their ^{77}Se hyperfine data. Their analysis will be critically discussed further below. Earlier optical experiments[5]—see Wagner[6] for a review—clearly demonstrate the A_{1g} character of the chalcogen pair ground state, as will be shown later. Calculations by Weinert and Scheffler[10] also favor positive parity.

In this paper EPR and ^{33}S ENDOR measurements are presented that prove the trigonal symmetry of the sulfur pair with high experimental accuracy. The electron-spin value is confirmed to be $S=\frac{1}{2}$. The lack of delocalization with respect to isolated sulfur can be accounted for by an even ground state. A large quadrupole effect is reported, which provides an important experimental clue to the valence structure of chalcogen pairs.

II. EXPERIMENTAL

The isotopically enriched sulfur used in the experiment contained 25.54 at. % of the magnetic isotope ^{33}S, which has nuclear spin $I=\frac{3}{2}$, nuclear g value $g_N=0.4290$, and quadrupole moment $Q=-5.5\times10^{-30}$ m^2.[11] This was diffused into p-type, floating-zone silicon doped with about 5×10^{15} boron atoms per cm^3 and a room-temperature resistivity of 3 Ω cm. A 0.5-cm^3 quartz ampoule initially containing 0.5 mg S mixed with excess Si powder and a $2\times2\times20$ mm^3 crystal was kept at 1370 °C for a period of 40 h. Under these circumstances a 1-bar SiS atmosphere is formed.[12] The ampoule volume was small to prevent deterioration of the crystal by vapor transport. After the diffusion treatment the ampoule was cooled down to room temperature in about 2 min. The magnetic-resonance experiments were carried out on a K-band superheterodyne spectrometer operating at 23 GHz. The magnetic field was modulated at a frequency of 83 Hz. The radio frequency (rf) signal for ENDOR measurements was chopped at a rate of 3.3 Hz. For a complete description, see Sprenger.[13] The field-scanned ENDOR (FSE) technique was described by Niklas and Spaeth.[14] The usual procedure for ENDOR measurements is to lock the magnetic field on the EPR line while scanning the rf, which produces a nuclear-magnetic-resonance- (NMR-) like spectrum. In FSE one locks the

rf to an NMR line and then the magnetic field is scanned. The observed ENDOR spectrum in this case looks like ordinary EPR, but only EPR transitions connecting levels involved in the NMR transition are observed. Thus FSE allows the study of unresolved EPR features.

III. RESULTS

At temperatures between 10 and 20 K, the EPR spectra of isolated sulfur (S^+) and the sulfur pair (S_2^+) are observed. The absolute and relative intensities of these spectra depend strongly on the thermal treatment. Samples cooled down to room temperature at a moderate rate, in about 2 min, showed strong S_2^+ and relatively weak S^+ resonances. Subsequent rapid quenching in water from about 1200 °C resulted in a sharp rise of the S^+ resonance accompanied by a drop in the S_2^+ intensity. A short treatment at 800 °C, followed by a rapid quench in water, undid the effect of the 1200 °C quench. At temperatures below or above 800 °C the S_2^+ signal did not regain its original intensity. One concludes that the pairs dissociate above 800 °C, whereas they are converted into nonparamagnetic higher-order complexes below this temperature. The pairs are seen to be rather stable.

The pair spectrum is shown in Fig. 1. It consists of a central line ($I=0$), a fourfold spectrum ($I=\frac{3}{2}$) due to ^{33}S-S centers, and a sevenfold spectrum due to ^{33}S-^{33}S, which can be regarded as a superposition of spectra with $I=0$, 1, 2, and 3. The relative intensities of the spectra are consistent with a ^{33}S abundance of 25% and two equivalent sulfur sites. Precise position measurements on the ^{33}S-S spectrum for $\mathbf{B}\|[100]$ reveal a slight deviation from equidistance. This is due to higher-order mixing of the quadrupole and the hyperfine interaction, as will be shown next. The spectra will be described by the spin Hamiltonian

$$H=\mu_B\mathbf{B}\cdot\vec{g}\cdot\mathbf{S}-g_N\mu_N\mathbf{B}\cdot\mathbf{I}+\mathbf{S}\cdot\vec{A}\cdot\mathbf{I}+\mathbf{I}\cdot\vec{Q}\cdot\mathbf{I}\,, \tag{1}$$

with nuclear spin $I=\frac{3}{2}$. At this point trigonal symmetry and electron spin $S=\frac{1}{2}$ will be assumed. A definite determination of the symmetry and the electron spin will be made further on. For $\mathbf{B}\|[100]$ the EPR transitions are, up to second order, given by

$$\begin{aligned}
h\nu&=g_{xx}\mu_B B+\tfrac{3}{2}A_{xx}+\tfrac{3}{4}A_{xx}^2/g_{xx}\mu_B B+30Q_{xy}^2/A_{xx}\,,\\
h\nu&=g_{xx}\mu_B B+\tfrac{1}{2}A_{xx}+\tfrac{7}{4}A_{xx}^2/g_{xx}\mu_B B-18Q_{xy}^2/A_{xx}\,,\\
h\nu&=g_{xx}\mu_B B-\tfrac{1}{2}A_{xx}+\tfrac{7}{4}A_{xx}^2/g_{xx}\mu_B B+18Q_{xy}^2/A_{xx}\,,\\
h\nu&=g_{xx}\mu_B B-\tfrac{3}{2}A_{xx}+\tfrac{3}{4}A_{xx}^2/g_{xx}\mu_B B-30Q_{xy}^2/A_{xx}\,.
\end{aligned} \tag{2}$$

Second-order contributions from the (in EPR) unresolved anisotropies g_{xy} and A_{xy} may be neglected. From Eq. (2) and the accurate EPR positions, not only g_{xx} and A_{xx}, but also Q_{xy} can be determined. The result is $Q_{xy}=2.46$ MHz, whereas a computer fit, based on diagonalization of Eq. (1) with g_{xy} and A_{xy} put to zero, gives $Q_{xy}=2.43$ MHz. Although the quadrupole effect is purely nuclear, its magnitude can thus be obtained from EPR. As will be seen in Sec. V, a fully occupied sulfur p orbital gives rise to a quadrupole effect of $Q_{\|}\simeq 10$ MHz. Since the pair contains two extra valence electrons, the quadrupole splitting may be as large as 40 MHz. Therefore the accurate EPR analysis greatly facilitated the search for ENDOR.

At a temperature of 18 K ^{33}S ENDOR could be observed. An example of an ENDOR spectrum is shown in Fig. 2. The linewidth is typically 25 kHz. As the hyperfine spectrum is well resolved in EPR, the NMR transition to which an observed resonance corresponds can be identified from observations of this resonance alone, without knowledge of the full angular pattern. Consider the level scheme shown in Fig. 3. If, e.g., an ENDOR line is observed only for B positioned on the $m_I=\frac{1}{2}$ and the $m_I=\frac{3}{2}$ EPR line, it is one of the transi-

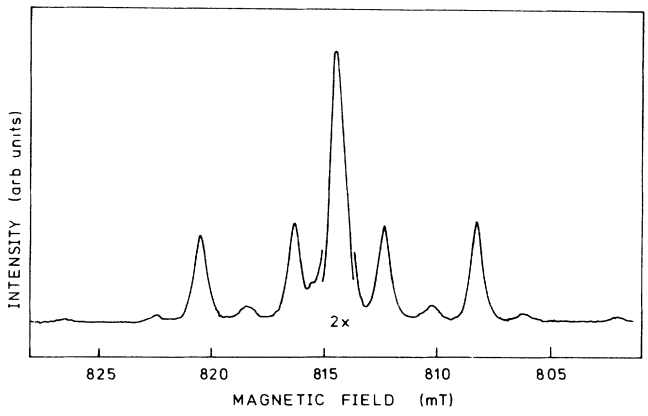

FIG. 1. The EPR spectrum of the sulfur pair for $\mathbf{B}\|[100]$, recorded at a microwave frequency of 22.8144 GHz and at a temperature of 18 K. Due to the 25% enrichment in ^{33}S, the spectrum is a superposition of S_2^+ ($I=0$), (^{33}S-S)$^+$ ($I=\frac{3}{2}$), and $^{33}S_2^+$ ($I=0,1,2,3$) resonances. The $^{33}S_2$ spectrum is a set of lines with $m_I=0$, ±1, ±2, and ±3 with relative intensities of 4, 3, 2, and 1, respectively. The single sulfur resonance is not observed at this temperature.

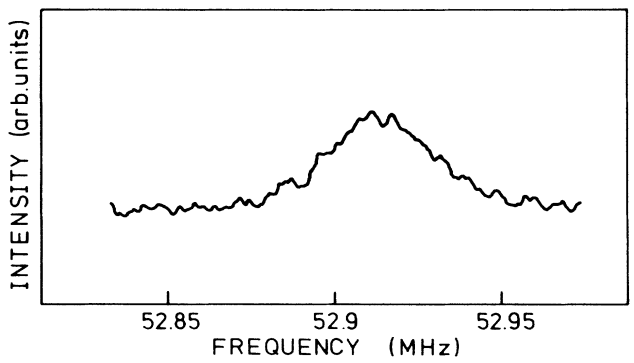

FIG. 2. Example of a ^{33}S ENDOR spectral line with $\mathbf{B}\|[100]$. Transition $|\frac{1}{2},-\frac{1}{2}\rangle\leftrightarrow|\frac{1}{2},+\frac{1}{2}\rangle$. The width is about 25 kHz.

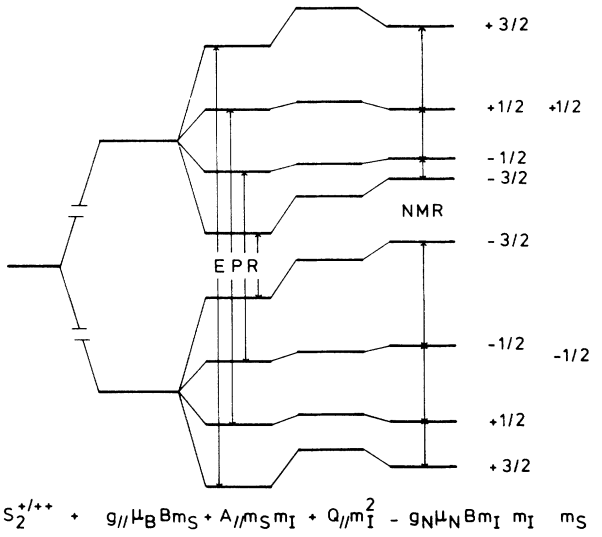

FIG. 3. Level scheme for the spin Hamiltonian of Eq. (1). The EPR transitions ($\Delta m_S = \pm 1, \Delta m_I = 0$) and the NMR transitions ($\Delta m_S = 0, \Delta m_I = \pm 1$) are indicated. The figure was drawn for $B = 816$ mT and **B** along the defect axis. The expressions given for the splittings are exact in this case.

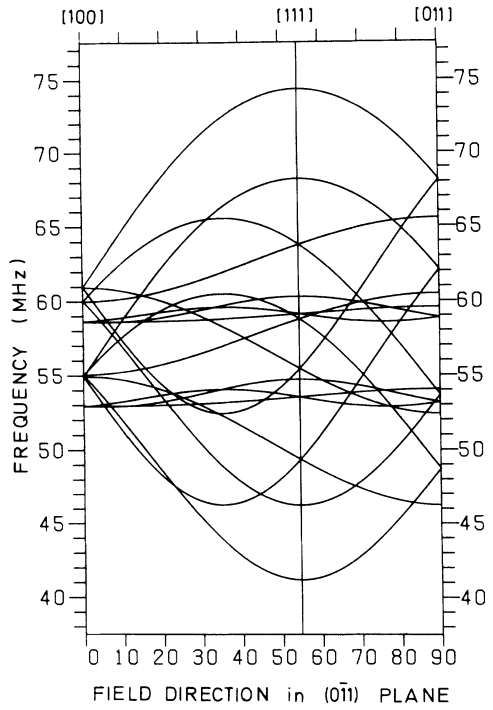

FIG. 4. Full angular dependence of the ^{33}S ENDOR spectrum of S_2^+, as calculated from the observed parameters at a magnetic field of 808.32 mT and a microwave frequency of 22.8144 GHz. The observed resonances were all situated within 5 kHz from the displayed curves.

tions $|\pm\frac{1}{2},\frac{1}{2}\rangle \leftrightarrow |\pm\frac{1}{2},\frac{3}{2}\rangle$. A similar reasoning holds for the other NMR transitions. Since an NMR transition is observed at two different magnetic-field values and one has $h\Delta\nu = g_N \mu_N \Delta B m_S / |m_S| \simeq 13$ kHz, m_S can be determined from the sign of the frequency shift.

The observed ENDOR positions could be fitted to within 5 kHz with the Hamiltonian given in Eq. (1), with trigonal symmetry, $I = \frac{3}{2}$ and $S = \frac{1}{2}$. This fully establishes the symmetry and the electronic spin, since a higher electronic spin would have produced well-resolved second-order splittings. Inclusion of the higher-order terms of the type BSI^2, BI^3, and SI^3 did not improve the computer fit significantly. The resulting spin Hamiltonian parameters are shown in Table I. Also given is the value of g_{xy}, as determined from ^{29}Si field-scanned ENDOR (FSE), with **B**$\|[011]$.[15] For comparison, the corresponding values for the selenium pair[7] are also included.

The observed value of g_N agrees with the value of $+0.4290$ given by Fuller,[11] who also provided the g_N value of ^{77}Se. It is reasonable to assume that g_{xx} and A_{xx} are positive. Experimentally, Q_{xy} and A_{xx} are determined to have the same sign, which implies $Q_{xy} > 0$. Figure 4 displays the full ^{33}S ENDOR spectrum of the sulfur pair. The anisotropy is completely dominated by the large quadrupole splitting. The defect orientations in the magnetic-field plane, which correspond to the open loops in the figure, were not observed in ENDOR. The reason is that for **B** parallel to the defect axis the EPR intensity collapses, as can be seen from Fig. 5, which shows a detail of the EPR spectrum for magnetic field **B**$\|[111]$. For negative m_I the hyperfine and g anisotropies add up, and the resonance from the [111] pair orientation is separated from the coinciding $[1\bar{1}\bar{1}]+[\bar{1}1\bar{1}]+[\bar{1}\bar{1}1]$ resonances by about $+0.53$ mT, and is therefore just resolved in EPR. However, the EPR of the pairs aligned with **B** is only observed as a weak feature on the high-field flank of

TABLE I. Observed spin Hamiltonian parameters for S_2^+ and the corresponding values for Se_2^+ from Ref. 7.

Parameter	S_2^+		Se_2^+	
g_{xx}, g_{xy}	2.000 74(5)	−0.000 41(2)	2.0033	−0.0006
$g_{\|}, g_{\perp}$	1.999 92	2.001 15	2.0020(4)	2.0039(4)
g_N	0.4290(5)		1.0681	
A_{xx}, A_{xy} (MHz)	113.200(5)	0.878(5)	606(9)	6
$A_{\|}, A_{\perp}$ (MHz)	114.956	112.323	618(9)	600(9)
Q_{xy} (MHz)		2.300(5)		
$Q_{\|}, Q_{\perp}$ (MHz)	4.600	−2.300		

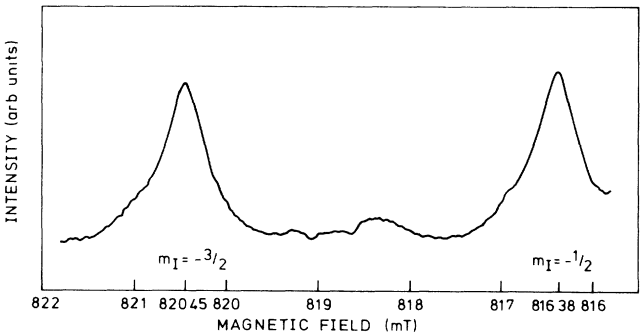

FIG. 5. Part of the EPR spectrum for $\mathbf{B}\|[111]$ at a microwave frequency of 22.8144 GHz. Shown are the $m_I = -\frac{3}{2}$ and $m_I = -\frac{1}{2}$ transitions. Three coinciding resonances contribute, belonging to the $[1\bar{1}\bar{1}]$, $[\bar{1}1\bar{1}]$, and $[\bar{1}\bar{1}1]$ defect orientations. The [111] orientation produces a barely visible shoulder on the high-field flanks.

the resonance from the nonaligned pairs. A possible explanation of this EPR collapse is that practically no orbital momentum parallel to the defect axis can be mixed into the ground state by spin-orbit interaction. Therefore, the spin-lattice relaxation in this case is strongly reduced. As a consequence, the EPR spectrum is determined by those pair orientations which are nearly at right angles to **B**, enhancing the isotropic appearance of the S_2^+ spectrum.

IV. THE DEFECT ELECTRON

The hyperfine interaction at the sulfur sites provides information about the defect electron. It will now be interpreted in terms of a linear combination of atomic orbitals (LCAO) treatment. The defect wave function Ψ is expanded in atomic orbitals ϕ_i situated at the lattice sites $\mathbf{R}_i$:

$$\Psi = \sum_i \eta_i \phi_i \ . \tag{3}$$

Restricting the basis set to s and p orbitals, one has at the sulfur site

$$\phi = \alpha\phi_s + \beta\phi_p \ , \tag{4}$$

where the site index has been dropped. Throughout the following, the formulas given by Sprenger *et al.*[16] for the hyperfine and quadrupole interactions of a p orbital will be used.

Following Morton and Preston,[17] an unpaired sulfur s orbital produces a contact interaction of $A_{xx} = 3463$ MHz, whereas an unpaired sulfur p orbital produces a hyperfine anisotropy of $A_{xy} = 100.5$ MHz. On comparing with the observed values of Table I, one finds $\eta^2\alpha^2 = 3.27\%$ and $\eta^2\beta^2 = 0.87\%$. The values of η^2, α^2, and β^2 for S_2 are compared to those of Se_2^+ in Table II.

In Table II hyperfine information was used from Refs. 2 (S^+), 5 (Se^+), and 7 (Se_2^+). The contact densities for the two pairs are very close and are proportional to the values for the isolated centers by nearly the same factor: 0.362 for S and 0.365 for Se. The total localization on both chalcogens practically equals the localization on the isolated chalcogen. This is not what one would expect, considering the S_2^+ center as a S^+ center, perturbed by a neutral S^0 on the nearest-neighbor site. For such a model the localization only equals that of the unperturbed S^+ center if ionization energies are equal. However, the pair is much shallower ($S_2^{+/2+} = 370.0$ meV) than the isolated defect ($S^{+/2+} = 613.2$ meV).[6]

TABLE II. LCAO parameters for sulfur and selenium centers calculated with atomic parameters from Ref. 17.

	S_2^+	Se_2^+	S^+	Se^+
$\eta^2\alpha^2$ (%)	3.27	3.01	9.03	8.25
$\eta^2\beta^2$ (%)	0.87	1.22		
η^2 (%)	4.14	4.23		
α^2 (%)	78.9	71.2		
β^2 (%)	21.1	28.8		

Surprisingly Wörner and Schirmer[7] conclude negative parity of the ground state from the observed reduction of the contact density of the pair with respect to the single defect. These authors did not take into account that Se_2^+ is considerably shallower than Se^+, which sufficiently explains the reduction, and neglected the contribution to the localization from the hyperfine anisotropy. Moreover, decisive experimental evidence for positive parity was already available—see, e.g., Ref. 5—when the Se_2 EPR spectrum was first reported. In Fig. 6 the multivalley split ground-state levels of isolated and paired sulfur are shown. In the case of S_2 the symmetry is lowered from $\bar{4}3m$ to $\bar{3}m$ and the T_2 triplet is split into an odd singlet A_{2u} and an odd doublet E_u. From Fig. 6 it is clear that the pair ground state is related to the S^+ A_1 state and therefore must be the even A_{1g} state. The possibility of an odd ground state can be excluded from these data.

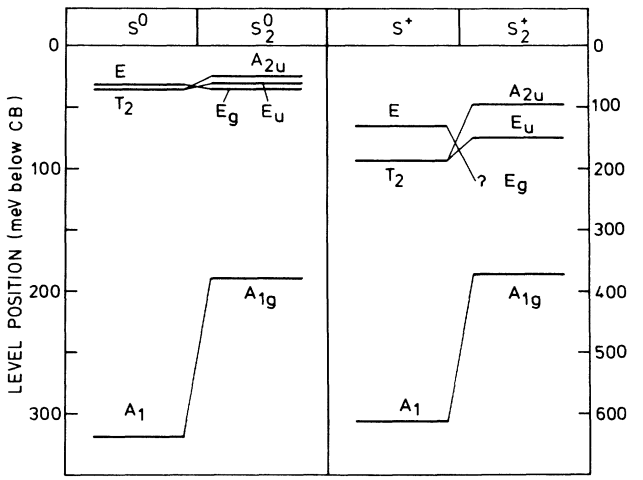

FIG. 6. Level scheme of 1s ground states of S^0, S_2^0, S^+, and S_2^+.

V. THE VALENCE ELECTRONIC STRUCTURE

The quadrupole interaction probes the charge distribution near the nucleus.[18] It reveals the deviation from tetrahedral symmetry of the valence electrons. If this deviation is small or no valence charge is present, as is the case for interstitials, contributions from defect electrons or unscreened nearby nuclear charges are also of importance. Direct information on the valence structure of a defect may be obtained from quadrupole effects.[19]

A positive elementary point charge situated at 2.35 Å from a ^{33}S nucleus along the [111] direction gives $Q_{xy}=-24.6$ kHz, using Eq. (12) of Ref. 16 and the nuclear data from Ref. 11. The unbalanced charge of a [111]-oriented sulfur $3p$ orbital leads to $Q_{xy}=+5.28$ MHz. Taking $\eta^2\beta^2$ from Table II, the defect electron contributes $Q_{xy}=+46.1$ kHz. Neglecting these contributions, the observed value of $Q_{xy}=+2.300(5)$ MHz corresponds to a valence charge unbalance of 44% of a sulfur $3p$ electron on the defect axis.

Each sulfur contributes five valence electrons. Let us put four electrons in s-p hybridized bonds with the three Si and one S neighbor atoms. These may contribute to the quadrupole effect since S is more electronegative than Si, but this will be neglected here. Then the quadrupole moment should be produced by the remaining electron. This electron cannot be in an s orbital, since these are occupied and produce no quadrupole interaction.

One possibility is that the extra electron is in a $3p$ orbital oriented along the defect axis. This is equivalent to the sulfur having sp^2 bonds with its silicon neighbors and a lone pair of localized nonbonding p electrons along the defect axis. Since the valence unbalance does not correspond to an entire $3p$ electron, the extra electron should spend some of its time on the S—Si bonds as well. The S—S bond, and to a lesser extent also the Si—S bond, are weaker than pure sp^3 bonds in this model. Weinert and Scheffler[10] have found that the highest defect-related valence state has A_{2u} symmetry and is related to the A_{2u} valence state of the divacancy. They find a binding energy of -0.3 eV, which appears to be too small to explain the stability of the pair. As discussed above, the pairs are stable at temperatures up to at least 800 °C. A possible mechanism for increasing the binding energy is relaxation of the sulfur atoms along the defect axis. Such relaxation is consistent with the planar sp^2 character of the S—Si bonds in the model. Calculations that allow for lattice relaxation have been performed on several T_d symmetrical substitutional impurities in Si and GaAs,[20] among others Si:S, but not for defects of lower symmetry.

An alternative model is conceivable with the fifth electron in a d orbital. No value for $\langle r^{-3}\rangle_{3d}$ for sulfur is available, to our knowledge, but a fully occupied $A_{1g}(3d)$ orbital can account for the quadrupole effect, if one assumes $\langle r^{-3}\rangle_{3d}=0.6\langle r^{-3}\rangle_{3p}$. Calculations by Singh *et al.*[21] demonstrate the importance of d orbitals for neutral isolated chalcogens in silicon. It is well known that d orbitals are important in the chemistry of S, Se, and Te. For sulfur the energy required for $3p$-$3d$ promotion (8.4 eV) and $3s$-$3p$ promotion (7.9 eV) (Ref. 22) is comparable and it tends to form strong sp^3d^2 bonds in compounds like SF_6 and S_2F_{10}.[23] Finally, the involvement of d orbitals in S-, Se-, and Te-related defects in Si could explain why oxygen, which lacks low-lying d-orbitals, behaves so very differently from the heavier chalcogens. On the other hand, size effects may also be important.

VI. THE g TENSOR

Deviations of the g tensor of orbital singlets from the free-electron value $g_e=2.002\,32$ occur by admixture of orbital excited states through spin-orbit coupling. The g shift due to spin-orbit coupling at a specific shell of sites is given by[24]

$$g_{ij}-g_e=2\lambda\sum_{n\neq 0}\frac{\langle\phi_0|L_i|\phi_n\rangle\langle\phi_n|L_j|\phi_0\rangle}{E_0-E_n}\ . \tag{5}$$

The effect of the potential, i.e., the defect atomic potential or the ligand potential, is accounted for by the effective spin-orbit parameter λ. In this equation, the orbital moment is defined with respect to the ligand site under consideration. Consider an A_1 state in $\bar{4}3m$ symmetry, or an A_{1g} state in $\bar{3}m$ symmetry with **B** parallel to the axis. In these cases only orbital matrix elements with states of T_1 symmetry are nonvanishing. The nearest T_1 states are the excited $np_\pm$ states.[25] These are very shallow effective-mass states, the lowest of which, $2p_\pm$, is situated at 25.6 meV below the conduction-band edge. Moreover, only the nonspherical part of the ground state contributes, i.e., $l\geq 3$ for $\bar{4}3m$ and $l\geq 4$ for $\bar{3}m$ symmetry. This fact, combined with the large energy separation and difference in localization of the ground and the T_1 excited state, results in a very small g shift.

Since S- and Se-related centers have very similar electronic structure, the ligand contribution will be practically equal for both chemical species. However, the impurity contributions for the two atoms are expected to differ substantially. From atomic data[22] one finds $\lambda_{Se}=5\lambda_S$. It is therefore tempting to conclude from the near equality of the g values of S^+ and Se^+ that the impurity contribution is negligibly small. Schirmer and Scheffler[26] have proposed a model that predicts a linear, impurity-independent correlation between the g shift and the level position for orbital singlet states in cubic and axial symmetry. The model, apparently, is not valid for the chalcogen pairs, since there is a relatively large difference between the values of $g_\parallel$ for S_2^+ and Se_2^+ of 0.0021. As the hyperfine interactions at the impurity site indicate a remarkable similarity of the electronic structure for both defects, the g values indicate, contrary to the basic assumption of the model, that the impurity contribution cannot be neglected.

The fact that the EPR intensity is strongly reduced for **B** along the pair axis indicates that the spin-lattice relaxation, and therefore the spin-orbit coupling, should practically vanish for this case. But then $g_\parallel$ should be equal to the free-electron value, as is the case for Se_2^+ for which the relaxation effect is less drastic. Therefore the $g_\parallel$ shift of S_2^+, apparently, cannot be explained in the usual way.

The g anisotropy arises from spin-orbit coupling with the $1s(E_u)$ excited state. This is easiest seen for Se_2^+.

Since $\lambda_{Se}<0$ and $E_n>E_0$, one expects $g_\perp>g_e$, as is observed. The problems encountered in Ref. 7 can be traced to the fact that their Eq. (5) has the wrong sign.[27] The g anisotropy of S_2^+ can be understood in the same way, provided one considers $g_\perp-g_\parallel$, instead of $g_\perp-g_e$. The fact that the g anisotropy of Se_2^+ exceeds that of S_2^+ by only 50% can be understood by assuming that the impurity site contributes only 10% and the ligands 90%.

VII. SUMMARY AND CONCLUSION

The apparent isotropy of the S_2^+ EPR spectrum originates from a pronounced drop in EPR intensity, presumably caused by an increase in the relaxation time, for magnetic-field directions close to the defect axis direction. From the ^{33}S ENDOR spectrum it follows that the pair has trigonal ($\bar{3}m$) symmetry and $S=\frac{1}{2}$. The hyperfine interaction is consistent with even parity and demonstrates a close analogy of the sulfur and the selenium pair. Two electronic models are possible that explain the observed quadrupole interaction. The first has lone pairs oriented along the pair axis and sp^2 hybridized S—Si bonds. In this model, lattice relaxation has to be invoked in order to explain the pair stability. The second model has an A_{1g} state made up from $3d$ orbitals, corresponding to an extra sulfur bond. Calculations that allow for lattice relaxation and include sulfur d orbitals are required to decide between the two models. The g anisotropy of the chalcogen pairs is qualitatively understood as resulting from spin-orbit admixture of the excited $1s(E_u)$ state to the A_{1g} ground state.

ACKNOWLEDGMENT

This work received financial support from the Foundation for Fundamental Research on Matter (FOM), The Netherlands.

[1]R. O. Carlson, R. N. Hall, and E. M. Pell, J. Phys. Chem. Solids **8**, 81 (1959).
[2]G. W. Ludwig, Phys. Rev. **137**, A1520 (1965).
[3]W. E. Krag, W. H. Kleiner, H. J. Zeiger, and S. Fischler, J. Phys. Soc. Jpn. Suppl. **21**, 230 (1966); W. E. Krag, W. H. Kleiner, and H. J. Zeiger, Phys. Rev. B **33**, 8304 (1986).
[4]D. L. Camphausen, H. M. James, and R. J. Sladek, Phys. Rev. B **2**, 1899 (1970).
[5]E. Janzén, R. Stedman, G. Grossmann, and H. G. Grimmeiss, Phys. Rev. B **29**, 1907 (1984).
[6]P. Wagner, C. Holm, E. Sirtl, R. Oeder, and W. Zulehner, in *Festkörperprobleme: Advances in Solid State Physics,* edited by P. Grosse (Vieweg, Braunschweig, 1984), Vol. XXIV, p. 191.
[7]R. Wörner and O. F. Schirmer, Solid State Commun. **51**, 665 (1984).
[8]J. R. Niklas and J. M. Spaeth, Solid State Commun. **46**, 121 (1983).
[9]F. Beeler, M. Scheffler, O. Jepsen, and O. Gunnarsson, Phys. Rev. Lett. **54**, 2525 (1985); F. Beeler, O. K. Andersen, O. Gunnarsson, O. Jepsen, and M. Scheffler, Comput. Phys. Commun. **44**, 297 (1987).
[10]C. M. Weinert and M. Scheffler, Mater. Sci. Forum **10-12**, 25 (1986).
[11]G. H. Fuller, J. Phys. Chem. Ref. Data **5**, 835 (1976).
[12]C. Holm, Ph.D. thesis, Ludwig-Maximilians-Universität München, 1981 (unpublished).
[13]M. Sprenger, Ph.D. thesis, University of Amsterdam, 1986 (unpublished).
[14]J. R. Niklas and J. M. Spaeth, Phys. Status Solidi B **101**, 221 (1980).
[15]A. B. van Oosten (unpublished).
[16]M. Sprenger, R. van Kemp, E. G. Sieverts, and C. A. J. Ammerlaan, Phys. Rev. B **35**, 1582 (1987).
[17]J. R. Morton and K. F. Preston, J. Magn. Reson. **30**, 577 (1978).
[18]G. D. Watkins, Phys. Rev. **155**, 802 (1967).
[19]A. B. van Oosten and C. A. J. Ammerlaan, Solid State Commun. **65**, 1039 (1988).
[20]M. Scheffler, Physica **146B**, 176 (1987).
[21]V. A. Singh, U. Lindefelt, and A. Zunger, Phys. Rev. B **27**, 4909 (1983).
[22]C. E. Moore, in *Atomic Energy Levels,* Natl. Bur. Stand. (U.S.) Circ. No. 467 (U.S. GPO, Washington, D.C., 1947).
[23]R. McWeeny, in *Coulson's Valence,* 3rd ed. (Oxford University Press, Oxford, 1979), p. 204.
[24]A. Abragam and M. H. L. Pryce, Proc. R. Soc. London, Ser. A **205**, 135 (1951).
[25]A. K. Ramdas and S. Rodriguez, Rep. Prog. Phys. **44**, 1297 (1981).
[26]O. F. Schirmer and M. Scheffler, J. Phys. C **15**, L645 (1982).
[27]M. H. L. Pryce, Proc. Phys. Soc. London, Sect. A **63**, 25 (1950).